

Article

# Conceptual Design and Preliminary Verification of Distributed Wireless System of Weigh-in-Motion

Yun Wang<sup>1</sup>, Lei Gong<sup>1</sup>, Bingde Bao<sup>2</sup>, Jianchao Pan<sup>3,4</sup>, Qian Feng<sup>3,4</sup>  and Rongqiao Xu<sup>3,4,\*</sup> <sup>1</sup> School of Mechanical Engineering, Hangzhou Dianzi University, Hangzhou 310018, China<sup>2</sup> Zhejiang EVTech Co., Ltd., Hangzhou 310018, China<sup>3</sup> Department of Civil Engineering, Zhejiang University, Hangzhou 310058, China<sup>4</sup> Zhejiang Provincial Engineering Research Center for Digital & Smart Maintenance of Highway, Hangzhou 310051, China

\* Correspondence: xurongqiao@zju.edu.cn

**Abstract:** In this paper, the concept of a distributed wireless system of weigh-in-motion is proposed. A wireless sensor for weigh-in-motion (WIM) based on piezoelectric materials is designed. The corresponding prototype for indoor testing is made according to the design. It aims to realize the main functions of dynamic pressure sensing, charge signal amplification and conversion, wireless signal transmission and reception, etc. The material properties of the mechanical properties and the piezoelectric properties in the analyses are provided in detail. Through the indoor test platform, the feasibility of the wireless sensor for WIM designed in this paper is preliminarily verified, which provides a basic tool for the realization of the distributed self-powered wireless system of WIM in the next step.

**Keywords:** weigh-in-motion; conceptual design; distributed system; wireless transmission



**Citation:** Wang, Y.; Gong, L.; Bao, B.; Pan, J.; Feng, Q.; Xu, R. Conceptual Design and Preliminary Verification of Distributed Wireless System of Weigh-in-Motion. *Appl. Sci.* **2023**, *13*, 2467. <https://doi.org/10.3390/app13042467>

Academic Editor: Luigi Pomante

Received: 6 December 2022

Revised: 27 January 2023

Accepted: 2 February 2023

Published: 14 February 2023



**Copyright:** © 2023 by the authors. Licensee MDPI, Basel, Switzerland. This article is an open access article distributed under the terms and conditions of the Creative Commons Attribution (CC BY) license (<https://creativecommons.org/licenses/by/4.0/>).

## 1. Introduction

The safety and efficiency of the transportation network are important for economic and social development. The overloading of vehicles has become a worldwide public problem. Over-limit and overloaded vehicles cause great harm to traffic safety, the environment, and road facilities. It greatly threatens the health of transportation infrastructure including roads, bridges, and tunnels, accelerates their performance degradation, shortens the service period, and even leads to the collapse of bridges, which seriously endangers the safety of lives and property. Real-time monitoring of the load capacity of vehicles on the road can effectively curb the spread and deterioration of this trend. It is also a necessary means for management departments to master the actual traffic load. Additionally, it helps to make decisions on the maintenance of transportation infrastructures for their normal operation.

The contradiction between real-time monitoring of vehicle loads and smooth transportation is solved by weigh-in-motion (WIM) technology. It obtains information on the speed and axial/wheel load of vehicles through sensors embedded in the road to test the contact forces between the tires and pavements (wheel load) while the car is in motion. The origin of WIM can be traced back to the 1960s. However, due to the limitations of hardware and algorithms, it has not been developed and promoted much until recently. In traditional WIM technology, force sensors are generally buried in the excavated structural layer of pavements or installed after burying the plate structure to acquire tire force acting on it [1,2]. Due to its electromechanical coupling characteristics, piezoelectric material has been widely used in all sorts of electronic components [3] and also applied to WIM sensors in earlier times [4–6]. Alavi et al. [7] evaluated the performance of piezoelectric WIM sensors. Papagiannakis et al. [8,9] carried out fatigue and other performance evaluations of piezoelectric WIM sensors both indoors and on site. Laquinta et al. [10] analyzed the end effect of piezoelectric WIM sensors numerically and experimentally, pointing out that

such sensors need to be supplemented to reduce measurement errors. White et al. [11] estimated the performance, especially the durability, of the piezoelectric WIM sensors using quartz. Sekula and Kolakowski [12] studied the analytical model and actual performance of the railway track WIM system based on piezoelectric sensors. Gajda et al. [13] analyzed the effect of temperature on the error of piezoelectric sensors through indoor and field tests. Vaziri et al. [14,15] analyzed the performance of WIM sensors using three piezoelectric materials, quartz, piezoceramic, and PVDF, through field measurement and discussed the influence of air temperature and vehicle speed on these three piezoelectric sensors. Zhang et al. [16] developed sensors for the WIM system based on the advantages of low-temperature sensitivity, high reliability, and simple structure of piezoceramic. Otto et al. [17] established the theoretical model of the strip piezoelectric WIM sensors considering the effect of pavement deformation and emphasized the importance of considering the viscoelastic characteristics of structural layers of asphalt pavements by comparing them with measured structures. Burnos and Rys [18] performed field observations of flexible asphalt pavements and discussed the impact on weighing results under vehicle speed and temperature variation. They explained that the distribution differences between vertical and horizontal stresses in the pavement structure primarily cause measurement errors.

Currently, these WIM sensors embedded in the road actually measure the wheel load which is directly applied on the sensors. However, in the motion state of actual vehicles, the vehicle vibration is caused by the defects of pavement deformation, smoothness, or pits; thus, the pressure that the wheels applied to the pavement measured by sensors is not static, but dynamic and affected by various factors. Therefore, the existing WIM system needs to be adjusted according to the parameters on site through actual vehicles [7,19]. Karamihas et al. [20] and Chen and Hong [21] also present a detailed discussion about the requirement of WIM for pavement smoothness. These works are to calibrate the parameters of the WIM system through on-site or indoor tests. In fact, the whole WIM system is actually regarded as a black box. Without establishing a real theoretical model of the WIM system, empirical calibration parameters have difficulties in promotion and application; hence, calibration parameters are specifically set for each WIM station. Xiang et al. [22] carried out a series of MTS tests to verify the theoretical model of the multi-layer structure of PZT sensors. The experiment results indicated that the loading frequency plays a prominent role in identifying the load magnitude. Moreover, the model of PZT sensors neglects the dynamic effects from the load which neglects the differences under the same application at different frequencies.

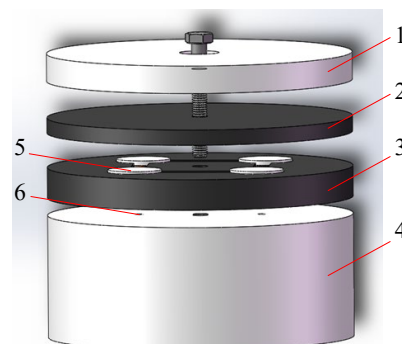
With the progress of electronic component technology, the self-powered wireless sensor technology is of great concern, which is achieved through harvesting energy from the surrounding environment [23,24]. At present, a lot of research focuses on micro/nano-devices for bioengineering [25]. With the development of artificial intelligence technology and its penetration into various fields, the concept of an intelligent expressway has been raised. Xiao et al. [26] proposed the concept of a self-powered wireless sensor applied to a smart pavement to monitor traffic flow. Hasni et al. [27] proposed a novel approach using a self-powered wireless sensor for the detection of bottom-up cracking in asphalt concrete pavements which can precisely inspect the entire process of the cracks' development. Agorastou et al. [28], through an integrated piezoelectric sensor interface, integrated signals based on the information of dynamic physical quantities and energy harvested to supply the sensors and implemented it on a simulated weigh-in-motion application. Panayanthatta et al. [29] utilized a piezoelectric transducer to convert the surrounding mechanical vibration energy into electrical energy, realizing a self-energy supply of sensors for wireless vibration monitoring. Obviously, this self-powered wireless sensor can greatly reduce the cost of battery replacements and make full use of the convenience brought by the rapid development of communication technology. It is also an important frontier technology in the field of intelligent transportation. This paper proposes a conceptual design of a self-powered WIM technology without damaging the road integrity. This phenomenon benefits from the electromechanical coupling characteristics of piezoelectric

materials to collect the road strain energy caused by traffic loads. Multiple sensors could also be arranged in the driving direction of vehicles to achieve the whole dynamic wheel load of driving vehicles. By optimizing the number and layout of sensors, machine learning could be used to analyze vehicle speed and axle load inversely [30], hence achieving a new type of distributed self-powered wireless WIM system.

## 2. Self-Powered Wireless WIM Sensor

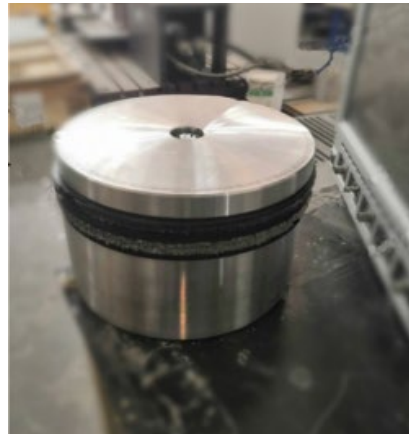
Traditional WIM systems are installed by excavating the road surface, positioning the sensors, and laying the power and signal transmission cables, which has a significant impact on traffic flow. The strain energy produced by the tire load of a moving vehicle is supposed to be absorbed by piezoelectric materials through the electromechanical coupling effect and converted into electrical energy to power a WIM system, making the sensor self-powered. Numerous works have been published in this field [23,24], and based on these discoveries, an energy-capture device is created, negating the need for power lines by meeting the demands of dynamic load cells for self-energy supply. In addition, wireless communication technology has been very mature. The test signals could be transmitted wirelessly, eliminating the need for signal transmission cables. It is important to further miniaturize the design to enable rapid deployment by using equipment for coring asphalt pavement rather than digging the road for traditional sensor replacement. Additionally, the coring device can be redesigned into a more practical shape for enhanced signal acquisition and energy capture.

Figure 1 depicts the self-powered wireless load cell's conceptual design. The cap, buffer layer, sensor layer, and base are the four components that make up the cylindrical sensor. The cap is subjected directly to the vehicle wheel load force, which is passed through the buffer layer to the sensor layer for energy capture and signal acquisition. Since the cap is immediately subjected to the vehicle's wheel stress and is exposed to a rather severe environment, it is essential that the cap has certain levels of tensile strength, stiffness, and durability. The buffer layer is designed to protect the sensor and energy capture device from excessive mechanical stresses. It is often composed of more durable material, such as rubber, and its thickness can be determined by testing. Core sensing and energy-capturing components of the complete sensor are supported by a sensing and energy capturing-layer with adequate strength and rigidity. By employing specialized equipment to drill holes in the pavement's construction layer, the entire sensor may be rapidly and easily installed without the need for power and signal lines. In order to remove it from the pavement construction layer for maintenance or replacement, specialized equipment must be constructed. Figure 2 shows a trial prototype with a 304 stainless steel lid, base, and rubber buffer layer. The sensing captive energy layer is composed of a multi-layer sandwich of rubber, in which the sensors and captives are arranged with a line groove of a specified width between them. In addition, the center of the 6mm diameter through-hole, the sensor, and the capturer can be inserted via the hole between the wires into the base.



1: Cap; 2: Buffer layer; 3: Sensor Layer;  
4: Base; 5: Sensor; 6: Hole for cables

**Figure 1.** Schematic diagram of a wireless WIM sensor.

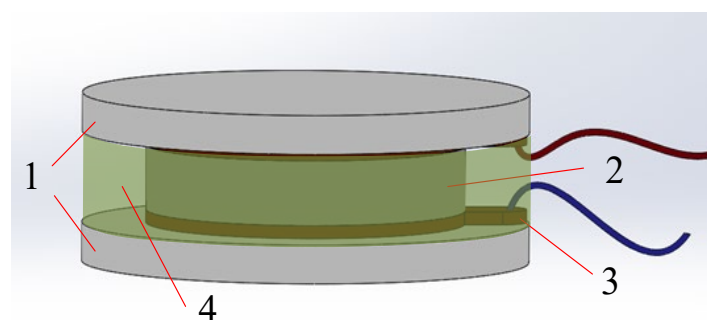


**Figure 2.** A prototype of a wireless WIM sensor.

The piezoelectric sensing and energy harvesting unit is designed as a disc structure, with a piezoelectric ceramic of PZT-8 (25 mm diameter, 10 mm aperture, and 5 mm thickness), two copper electrodes, two stainless steel gaskets, two wires, and external room temperature curing silicone rubber. The Piezoelectric properties of PZT-8 are listed in Table 1. The detail of the structure is shown in Figure 3. Considering the brittleness of piezoceramics, brass electrodes with pins are used. Additionally, wires are welded on the pins of the brass electrodes, which can avoid the unevenness of electrode welding spots. A stainless-steel spacer slightly larger than the PZT piezoelectric ceramic sheet is used to prevent the piezoelectric material and electrode from the influence of external environments such as rain. A stainless-steel spacer with the dimension of  $\phi 35 \times 3$  mm is employed, which can be filled with flexible room-temperature cured silicone rubber on the side of the PZT piezoelectric sheet, thus avoiding lateral force. The piezoelectric piece and electrode piece are tightly combined with the stainless-steel gasket so that the piezoelectric ceramic piece is stressed uniformly in the polarization direction as far as possible. Figure 4 shows the sample that was developed.

**Table 1.** Piezoelectric properties of PZT-8.

PZT-8	Electric Capacity	Wastage (tan $\delta$ )	Frequency	Reverse-Frequency	Bandwidth	Impedance	Coupling Coefficient	Quality Factor
$\Phi 25 \times \Phi 9.5 \times 5$ mm	943 pF	0.3%	61.1 kHz	65.9 kHz	4.9 kHz	14.2 $\Omega$	60%	1000



1: stainless steel gasket; 2: PZT;  
3: copper electrode; 4: cured silicone rubber

**Figure 3.** Structure of piezoelectric sensing unit.

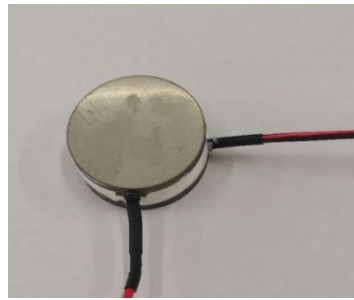


**Figure 4.** A prototype of piezoelectric sensing unit.

### 3. Design of Distributed WIM System

Due to the vertical vibration of the vehicle itself, as well as the deformation, unevenness, or defects of the road surface, the vertical vibration of the measured vehicle is caused. In this case, the wheel load of the vehicle (the pressure of the vehicle tires on the road surface) is dynamically changing with a certain periodicity. Obviously, the error between the dynamic wheel load and the vehicle weight is closely related to the vibration characteristics of the running vehicle. At present, most of the sensors arranged in the WIM system only install strip sensors in a narrow range of the vehicle's traveling direction. The time for the tires of the moving vehicle passing above the sensor is only about 0.01–0.1 s. The dynamic wheel load throughout the cycle of the change process cannot be detected. Furthermore, the results in the weighing system have to be calibrated on site. To make up for this shortcoming, we need to arrange multiple WIM sensors in the driving direction of the vehicle, but the existing WIM sensors are difficult to realize without breaking the integrity of the outer road surface. However, this arrangement can be conveniently implemented using the previously proposed self-powered wireless sensors for WIM. These kinds of sensors do not need to be slotted and wired under the pavement surface because of the self-powered energy and wireless signal transmission. Hence, it can be designed as spatially independent distributed sensors, arranged in a certain form on the lane (Figure 5). Through layout optimization, the best distribution form that meets the actual requirements can be obtained. Then, measuring the change of dynamic wheel load in the whole cycle would provide more reliable data for the calculation of static wheel load (vehicle weight) and more accurate identification of the vehicle wheelbase, axle number, and travel speed.

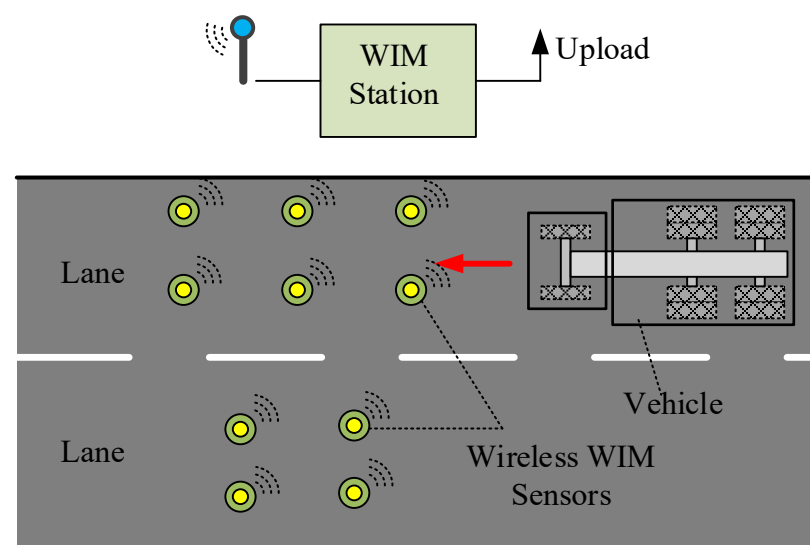


**Figure 5.** The schematic diagram of a distributed WIM system.

The schematic diagram of a distributed WIM system is shown in Figure 5. The wireless self-powered weighing sensors after optimization are distributed in the lane. When a sensor

detects the wheel load of a vehicle passing by, it records the change of the wheel load and transmits the data to the WIM station set at the roadside in real-time. After data processing, the WIM station obtains the vehicle speed, number of axles, axle load, and wheel load, and then uploads the information to the cloud database.

### 3.1. Charge Amplifier Circuit

When the wheel loads act on the wireless sensor for WIM based on piezoelectric materials, in order to detect the charge produced by piezoelectric quantitatively, a charge amplifier circuit is then introduced to transform it into the voltage signal, which can be collected easily. To successfully collect signals, the charge conversion circuit must satisfy the following requirements: (1) the output of the voltage signal is not sensitive to the external influence; (2) a high magnification is needed; and (3) the range of the measured frequency range should be wide enough. In summary, this paper adopted the OPA128 operational amplifiers, which are produced by TI company in America, as the core of the module. Additionally, its main technical indexes include (1) the maximum value of an ultra-low bias current of 75 fA, (2) the maximum value of an offset voltage of 500  $\mu$ A, (3) the temperature drift of 5  $\mu$ A/ $^{\circ}$ C, (4) the minimum value of a high open-loop gain of 110 dB, and (5) the minimum value of the high Common Mode Rejection (CMRR) of 90 dB. These performance indexes meet the use requirements of the charge-amplifying and conversion of the circuit in the signal measuring module of the vehicle WIM sensor.

Based on the chosen operational amplifiers, the charge-amplifying and conversion circuit has been designed with the circuit diagram shown in Figure 6. The generated signal frequency band between the vehicle and sensors may be high when the vehicle speed is high as well, so the OPA128LM was placed in parallel connection with the capacitor C10. Meanwhile, to protect the operational amplifier, a series connection was achieved with a resistor R8 in the input terminal of OPA128LM. Additionally, a capacitor C7 was connected in parallel to R8, which was intended to avoid another pole leaded by the input capacitance of OPA128 and R8. Finally, due to the great stress difference in each contact point, the stability of the output signal can be satisfied by adjusting the circuit gain. Based on the schematic figure of the charge-amplifying and conversion circuit, the corresponding circuit was made shown in Figure 7.

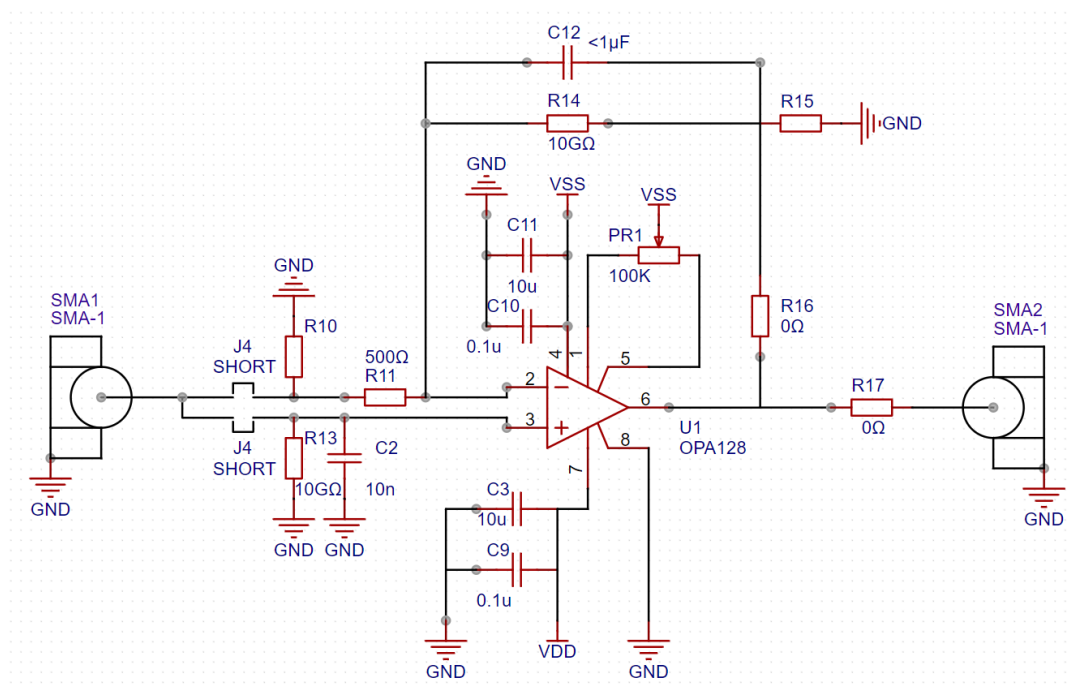


**Figure 6.** Circuit diagram of charge-amplifying and conversion.

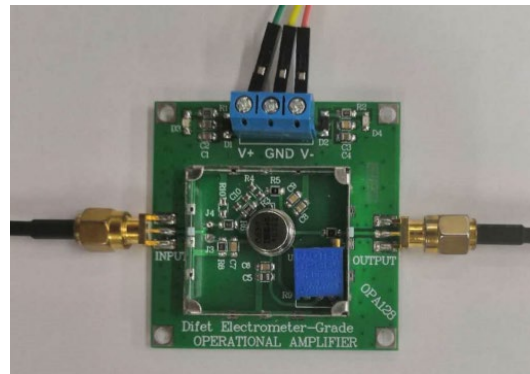


**Figure 7.** A prototype of charge-amplifying and conversion circuit.

### 3.2. Selection of Single-Chip Microcomputer

Experiments have shown that the contact time between the driving vehicles on the way and the sensor ranges from 0.01 to 0.1 s. Therefore, when choosing a single-chip microcomputer, it is necessary to consider whether it has sufficient sampling frequency, as well as power consumption and performance. Through comprehensive consideration, the single-chip microcomputer STM32F103RCT6 was chosen, and the widely-used kernel ARM cortex-M was adopted, which has the following characteristics: (1) with a 32-bit processor, it runs more efficiently than a single-chip microcomputer with only a 16-bit processor; (2) it includes 12-bit A/D converters; (3) it has faster data processing speed while the upper limit of its working frequency is 72 MHz; (4) it has small supply voltage ranging from 2 V to 6 V and low power consumption; (5) it has high integration, communication module, and other functional modules.

### 3.3. Wireless Transmission Module

Wireless data transmission technology is the key to realizing the routing without grooving under the pavement surface. The following requirements should be considered when selecting a wireless transmission module: (1) stability of data transmission should be included because it is very important for the signal generated by the sensor to be sent and received accurately, considering data loss will cause the measurement error of the whole system; (2) the data transmission distance should be relatively long to meet the requirements of sending and receiving data of short and medium distance WIM sensor; (3) power consumption should be considered because the whole system can provide self-power, but the electricity provided will be very limited, so the wireless module needs to have the characteristics of low power consumption. By comparing the characteristics of existing wireless modules and combining them with the requirements of vehicle WIM system, this paper chooses the NRF24L01 wireless module, which mainly has the following characteristics: (1) high speed because the air transmission rate of NRF24L01 module can reach 2 Mbps, reducing the data transmission time and effectively avoiding the consumption of the signal itself in the transmission process; (2) low power consumption which means when the module is in response mode for communication, it can be transmitted and started quickly, greatly reducing the current consumption; (3) low operating voltage, which is to guarantee that the module can work normally under the voltage provided by STM32 MCU; (4) automatic retransmission function, which is to effectively prevent the omission of signals in the process of wireless data transmission.

According to the design requirements and referring to the usage document of NRF24L01, the wireless transmission module is designed here. In order to facilitate the connection with the STM32 module, the SPI interface is reserved, as shown in Figure 8, to achieve the purpose of wireless data transmission. Figure 9 shows a prototype of the wireless transmission module.

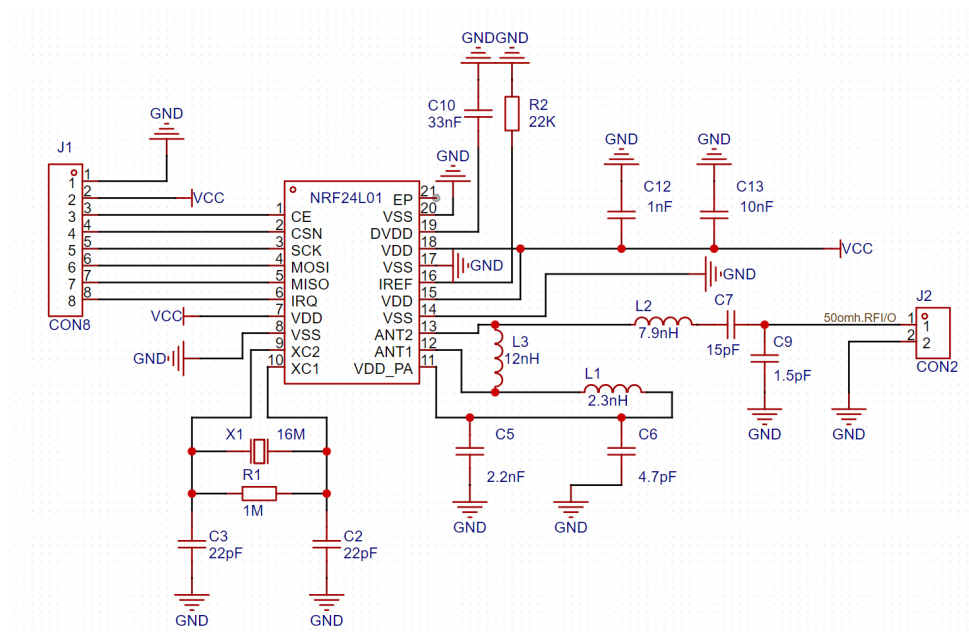


**Figure 8.** Circuit diagram of NRF24L01.

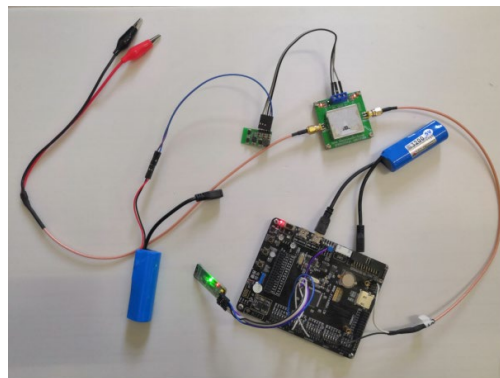


**Figure 9.** A prototype of wireless transmission module.

### 3.4. Hardware Circuit Design

The system's OPA128 charge conversion amplifier needs  $\pm 5$  V power supply. In order to convert the operating voltage of STM32 MCU 3.3 V to  $\pm 5$  V power supply for the OPA128 charge conversion amplifier, a voltage conversion module needs to be added. Figure 10 is the designed circuit schematic diagram. As can be seen from the schematic diagram, this paper adopts an XL6008 power supply booster chip, combined with 78M05 and 78M06 three-terminal voltage regulator chip, which uses 78M05 to stabilize +5 V voltage and 78M06 to stabilize  $-5$  V voltage, and finally converts the input DC voltage to  $\pm 5$  V voltage. The XL6008 power boost chip was chosen because it has a wide voltage input range, accepting 3.6 V–32 V input voltages. The 78 M series can operate at a voltage input of 35 V. The minimum input and output voltage difference, which is the instability voltage value, is 2 V. As shown in Figure 10, in order to suppress self-excited oscillation, an output filter capacitor is designed. The positive terminal of the capacitor is connected to a 78M05/78M06 output. The negative terminal is connected to the power source. Meanwhile, in order to prevent the situation of the input voltage from being less than the output voltage when the whole circuit stops supplying power, a diode is designed to ensure the safety of the circuit. The physical circuit is shown in Figure 11 of 5 V to  $\pm 5$  V.



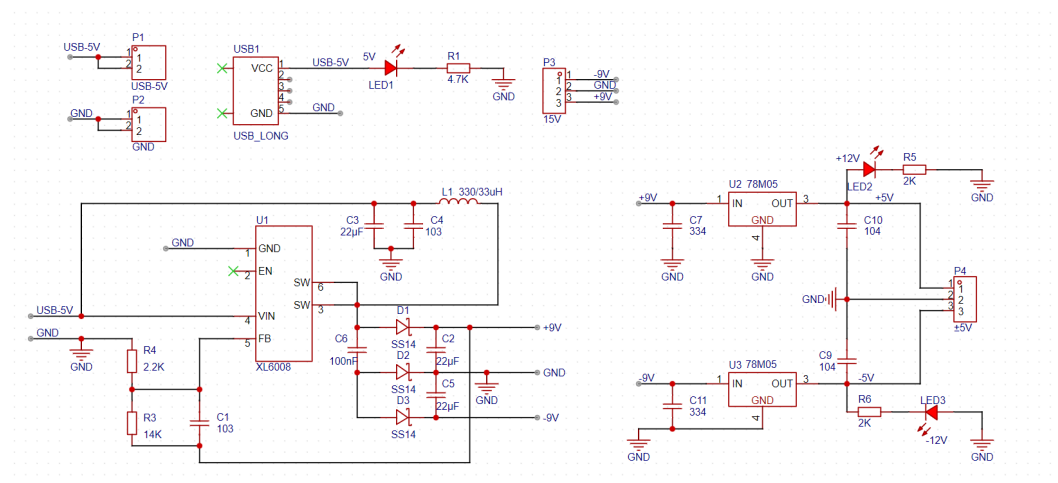


Figure 10. Circuit diagram of 2.8 V–9 V to  $\pm 5$  V.

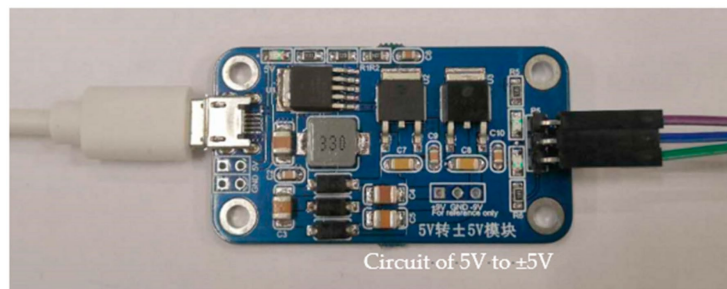


Figure 11. A prototype of circuit.

#### 4. Preliminary Validation

##### 4.1. Piezoelectric Sensing Unit Verification

Four piezoelectric sensor units make up the entire system of vehicle weigh-in-motion. Therefore, each sensing unit needs to be evaluated and validated before the viability of the entire weighing system is tested. The impact load test is created to confirm the sensing unit’s viability. The constructed test platform is shown in Figure 12. The main experimental test instruments used are shielding boxes, computers, 6517B electrostatic meters/high resistance meters, data acquisition cards, etc.

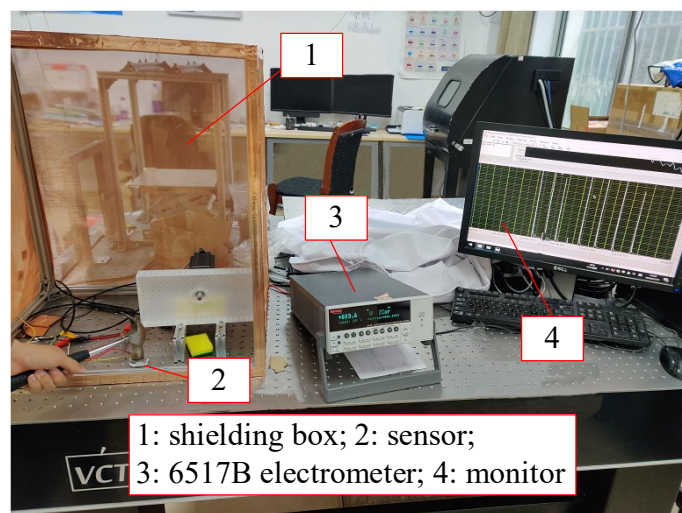


Figure 12. The platform for sensing unit test.

A 10 KG weight is put on the sensor in the sensitivity measurement experiment, and the pressure is altered by pushing the hand on the weight. The relationship between the voltage and the pressure is shown in Figure 13. The acquired data interface shows that the impact load induced by applying the weight causes the sensor to swiftly develop a voltage peak. After the impact load is removed, the voltage change curve progressively becomes steady. The voltage signal that the sensor outputs varies quickly as the load changes. The voltage recovers to its value in the static load condition once the external force is withdrawn and is typically steady. As a result, it can be seen that our sensor has great sensitivity and a quick reaction time.

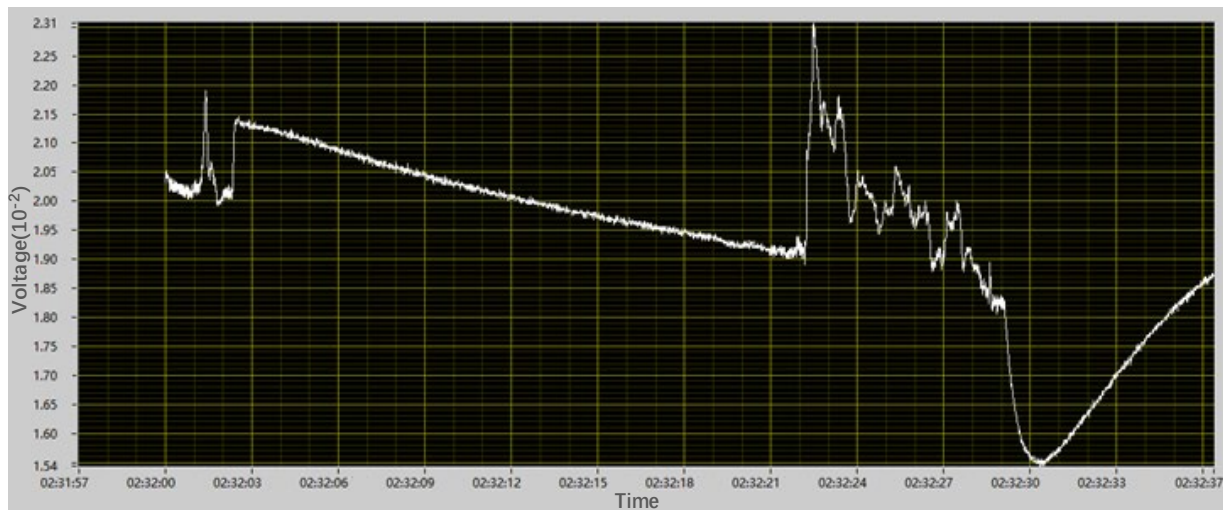


Figure 13. Output voltage.

The sensor and vehicle make contact for around 0.1 s; hence, it is important to confirm the sensor's properties under impact load. The voltage change curve of the sensor under impact load is shown in Figure 14.

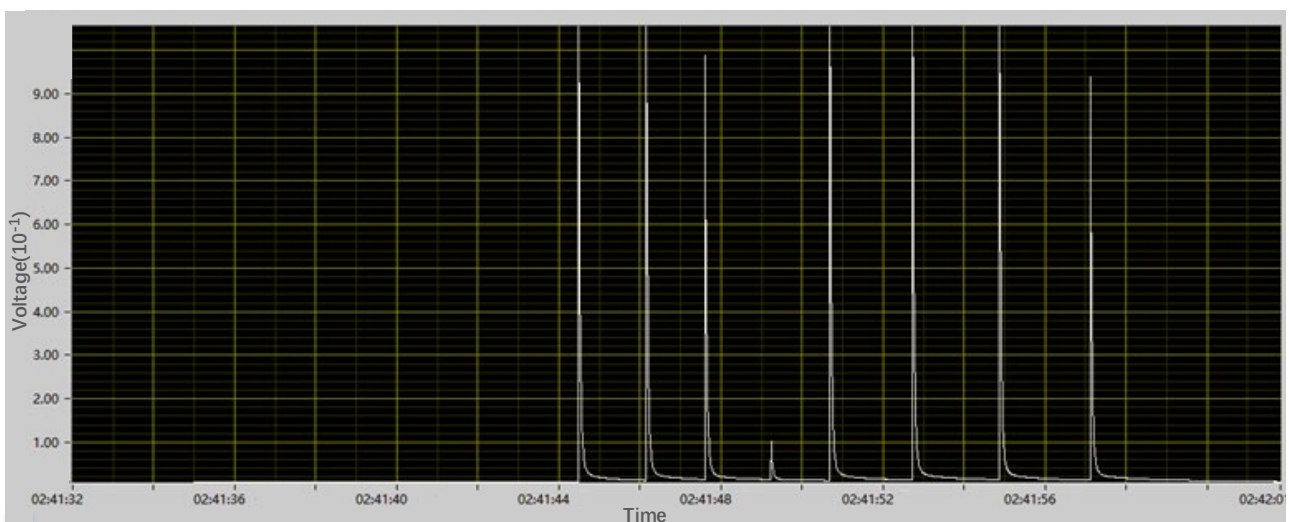


Figure 14. Sensor voltage curve under impact load.

The obtained data interface shows that the voltage value almost tends to zero and keeps aligned in the absence of an impact load. When the impact load is applied to the sensor, a sharper voltage peak is formed. Meanwhile, it is apparent that the voltage peak varies more dramatically for impact loads of various sizes.

In summary, it can be stated that the sensor proposed in this work fulfills the scheme's requirements since it has quick reaction times, high sensitivity, and the ability to create a relatively visible peak voltage when subjected to impact loads.

#### 4.2. Testing of the Wireless WIM Sensor

In order to apply the dynamic load to the outside of the whole weighing sensor, an experimental platform as shown in Figure 15 has been built, including the following main instruments: hydraulic high-performance universal testing machine, charge amplifier, wireless transmitter receiver, computer, etc.

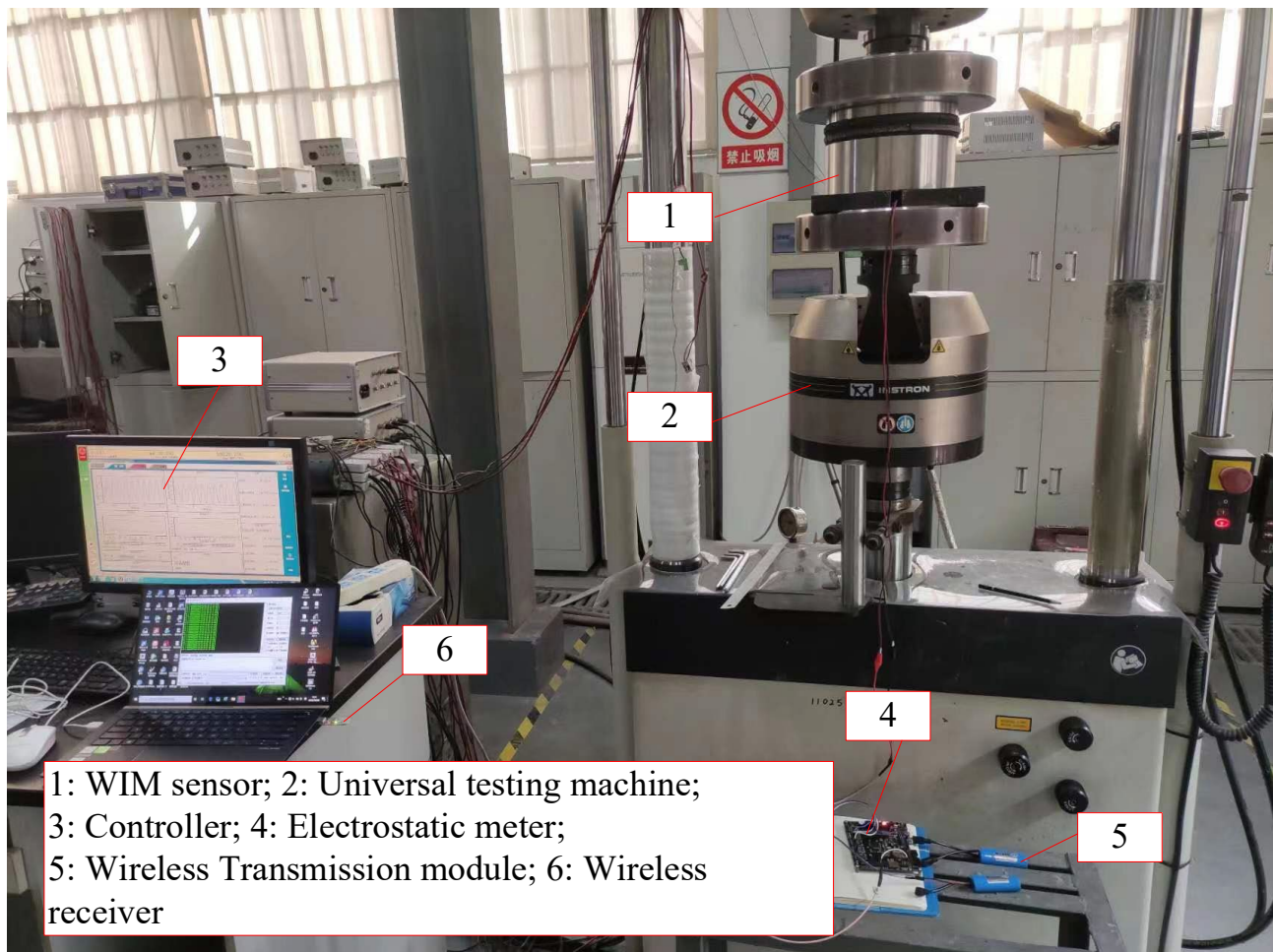


**Figure 15.** Establishment of dynamic load test platform.

As the maximum value of load in experiments is 80 kN, the diameter of the wireless WIM sensor is set to 200 mm, so the maximum crushing stress should be less than 2.5 MPa, to make sure not to exceed the maximum stress. The mechanical properties of WIM are listed in Table 2.

**Table 2.** Mechanical properties of WIM.

Materials	Young's Modulus	Poisson's Ratios	Yield Strength
304 Stainless Steel	190 GPa	0.3	$\geq 205$ MPa
PZT	90 GPa	0.3	$\geq 25$ MPa

By changing the dynamic load applied by the hydraulic universal testing machine, the size and stability of the signal output of the WIM sensor under different load conditions are

investigated. The output frequency of the testing machine is set as 5 Hz, and the peak loads are the cyclic loads with peak loads of 20 kN, 50 kN, and 80 kN, respectively. The obtained peak voltages are 320 mV, 713 mV, and 1178 mV, respectively, and the voltage waveform is shown in Figure 16. The comprehensive data analysis shows that the peak voltage changes linearly with the dynamic load, and the output signal is stable. The mechanical properties of WIM are listed in Table 2.

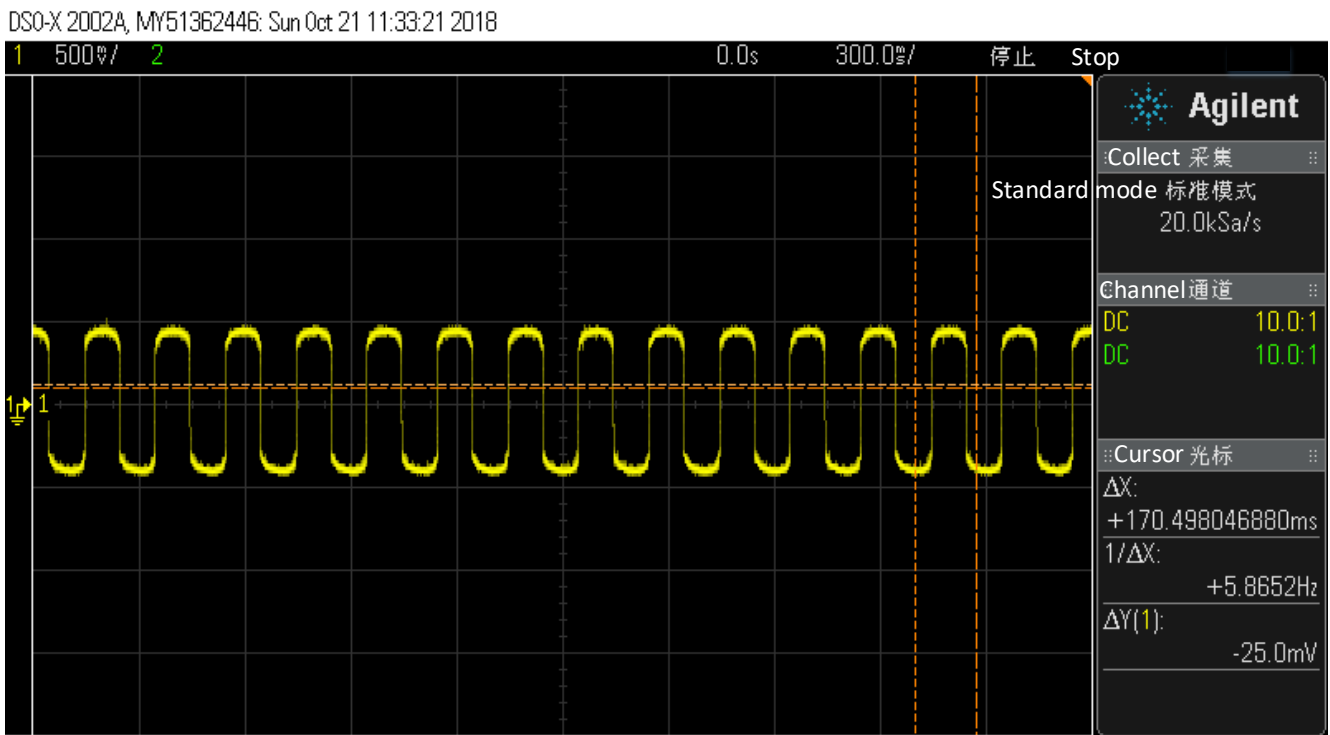


Figure 16. Curve of voltage output.

#### 4.3. Calibration of WIM Sensor

The weight of the vehicle is simulated by the applied load on the testing machine platform. A total of eight groups of experiments are conducted. The applied loads are 5 kN, 10 kN, 15 kN, 20 kN, 25 kN, 30 kN, 35 kN, and 40 kN, respectively. Each group of the applied loads is conducted several times in the experiment, and a linear relation is built between voltage and force. Hence the calibrated value can be obtained by converting the collected voltage. The experimental data and processed data are listed in Table 3 (the calibrated value is obtained by converting the collected voltage). In these eight experiments, the maximum relative error of the WIM sensor is less than 7%.

Table 3. WIM test data.

Applied Load (kN)	Measured Load (kN)	Absolute Error (kN)	Relative Error (%)
5	5.342	0.342	6.83
10	10.345	0.345	3.45
15	14.637	−0.363	2.42
20	20.180	0.180	0.90
25	24.513	−0.488	1.95
30	30.690	0.690	2.30
35	34.716	−0.284	0.81
40	40.092	0.092	0.23

## 5. Conclusions

In this paper, the conceptual design of distributed self-powered wireless system of WIM is proposed. A new wireless sensor for the WIM of road vehicles based on piezoelectric ceramics is designed and fabricated to measure the dynamic load of vehicles under normal driving conditions on the road. The collected signal is transmitted to the weighing station through a wireless transmission module. The main research work and results of this paper are as follows:

- (1) PZT piezoelectric ceramics were selected as the sensing material. The pressure sensing element was designed and fabricated in parallel to improve the piezoelectric output. The mechanical structure of the vehicle WIM sensor was also designed according to the requirements of the weighing sensor equipment on the road;
- (2) The circuitry required for the WIM sensor was designed and the prototype was built. It mainly consists of the charge conversion amplifier with a filtering function, the power supply circuit, and the A/D conversion function programmed using the STM32f103rct6 microcontroller. Meanwhile, the STM32f103rct6 microcontroller was combined with the wireless RF module NRF24L01 to realize the wireless transmission and reception of pressure signal data;
- (3) The signal response of the wireless WIM sensor under cyclic loads peaking at 20 kN, 50 kN, and 80 kN was verified by a high-performance universal testing machine. Preliminary results show that the mechanical and circuit design of the whole structure is reasonable and effective. It means the collected signals work well;
- (4) The piezoelectric sensing unit (Figure 3) can provide self-power (under the 5 Hz load of 20 KN, 50 KN, and 80 KN, respectively, the obtained peak voltages are 320 mV, 713 mV, and 1178 mV, respectively), but the electricity provided is very limited, which cannot provide the power of wireless transmission module (Figure 9). It means that the 'self-powered' module is conceptual at this stage and has not been totally realized yet.

The next step will be to implement the self-powered module with the road test. A new distributed self-powered wireless system of WIM would be optimized by adjusting the number and the arrangement of sensors. Machine learning would also be applied in the inverse analysis of vehicle travel speed and axle weight.

**Author Contributions:** Y.W.: Conceptualization, Methodology, Software, Validation, Investigation, Formal analysis, Visualization, Writing—original draft; L.G.: Conceptualization, Writing—Review & Editing, Funding Acquisition. B.B.: Conceptualization, Writing—Review & Editing, Funding Acquisition. J.P.: Conceptualization, Writing—Review & Editing. Q.F.: Conceptualization, Writing—Review & Editing. R.X.: Conceptualization, Methodology, Formal analysis, Writing—Review & Editing. All authors have read and agreed to the published version of the manuscript.

**Funding:** This work was supported by the "Pioneer" and "Leading Goose" R&D Program of Zhejiang (No. 2022C01143) and the National Natural and Science Foundation of China (Nos. 12072097, 12272335). This work was also supported by the ZJU-ZCCC Institute of Collaborative Innovation (No. ZDJG2022002).

**Conflicts of Interest:** The authors declare no conflict of interest.

## References

1. Michigan State Highway and Transportation Commission. *Automatic Weighing of Vehicles in Motion and Collection of Traffic Data by Electronic Methods*; Michigan State Highway and Transportation Commission: Lansing, MI, USA, 1974.
2. Machemehl, R.; Walton, C.M.; Lee, C.E. Acquiring traffic data by in-motion weighing. *Transp. Eng. J.* **1975**, *101*, 681–689. [[CrossRef](#)]
3. Wang, Y.; Xu, R.Q. State space formulation for magneto-electro-elasticity in Hamiltonian system and applications. *Compos. Struct.* **2015**, *133*, 607–620. [[CrossRef](#)]
4. Ali, N.; Trogdon, J.; Bergan, A. Evaluation of piezoelectric weigh-in-motion system. *Can. J. Civ. Eng.* **1994**, *21*, 156–160. [[CrossRef](#)]
5. Alavi, S.; Mactutis, J.; Gibson, S.; Papagiannakis, A.; Reynaud, D. Performance evaluation of piezoelectric weigh-in-motion sensors under controlled field-loading conditions. *Transp. Res. Rec. TRB* **2001**, *1769*, 95–102. [[CrossRef](#)]

6. Xiong, H.; Zhang, Y. Feasibility study for using piezoelectric-based weigh-in-motion (WIM) system on public roadway. *Appl. Sci.* **2019**, *9*, 3098. [[CrossRef](#)]
7. Papagiannakis, A. Calibration of weigh-in-motion systems through dynamic vehicle simulation. *J. Test. Eval.* **1997**, *25*, 197–204.
8. Papagiannakis, A.; Johnston, E.; Alavi, S. Fatigue performance of piezoelectric weigh-in-motion sensors. *Transp. Res. Rec. TRB* **2001**, *1769*, 87–94. [[CrossRef](#)]
9. Papagiannakis, A.; Johnston, E.; Alavi, S.; Mactutis, J. Laboratory and field evaluation of piezoelectric weigh-in-motion sensors. *J. Test. Eval.* **2001**, *29*, 535–543.
10. Iaquina, J.; Merliot, E.; Cottineau, L.; Desroche, J. Piezoelectric sensors for weigh-in-motion systems: An experimental insight into edge effects. *J. Test. Eval.* **2004**, *32*, 476–483. [[CrossRef](#)]
11. White, R.; Song, J.; Haas, C.; Middleton, D. Evaluation of quartz piezoelectric weigh-in-motion sensors. *Transp. Res. Rec. TRB* **2006**, *1945*, 109–117. [[CrossRef](#)]
12. Sekula, K.; Kolakowski, P. Piezo-based weigh-in-motion system for the railway transport. *Struct. Control Health Monit.* **2012**, *19*, 199–215. [[CrossRef](#)]
13. Gajda, J.; Sroka, R.; Zeglen, T.; Burnos, P. The influence of temperature on errors of WIM systems employing piezoelectric sensors. *Metrolog. Meas. Syst.* **2013**, *20*, 171–182. [[CrossRef](#)]
14. Vaziri, S.; Haas, C.; Rothenburg, L.; Haas, R. Investigation of the effect of weight factor on performance of piezoelectric weigh-in-motion sensors. *J. Test. Eval.* **2013**, *139*, 913–922.
15. Vaziri, S.; Haas, C.; Rothenburg, L.; Haas, R.; Jiang, X. Investigation of the effects of air temperature and speed on performance of piezoelectric weigh-in-motion systems. *Can. J. Civ. Eng.* **2013**, *40*, 935–944. [[CrossRef](#)]
16. Zhao, Q.; Wang, L.B.; Zhao, K.; Yang, H.L. Development of a novel piezoelectric sensing system for pavement dynamic load identification. *Sensors* **2019**, *19*, 4668. [[CrossRef](#)]
17. Otto, G.G.; Simonin, J.-M.; Piau, J.-M.; Cottineau, L.-M.; Chupin, O.; Momm, L.; Valente, A.M. Weigh-in-motion (WIM) sensor response model using pavement stress and deflection. *Constr. Build. Mater.* **2017**, *156*, 83–90. [[CrossRef](#)]
18. Burnos, P.; Rys, D. The Effect of Flexible Pavement Mechanics on the Accuracy of Axle Load Sensors in Vehicle Weigh-in-Motion Systems. *Sensors* **2017**, *17*, 2053. [[CrossRef](#)]
19. Sharma, S.; Stamatinos, G.; Wyatt, J. Evaluation of IRD-WIM-5000—A Canadian weigh-in-motion system. *Can. J. Civ. Eng.* **1990**, *17*, 514–520. [[CrossRef](#)]
20. Karamihas, S.; Rada, G.; Ostrom, B.; Simpson, A.; Wisner, L. Pavement smoothness at weigh-in-motion sites—Developing specifications for the long-term pavement performance program. *Transp. Res. Rec. TRB* **2004**, *1870*, 116–123. [[CrossRef](#)]
21. Chen, D.H.; Hong, F. Field Verification of smoothness requirements for Weigh-in-motion approaches. *J. Test. Eval.* **2009**, *37*, 40–47.
22. Tao, X.; Huang, K.; Zhang, H.; Zhang, Y.; Zhang, Y.; Zhou, Y. Detection of Moving Load on Pavement Using Piezoelectric Sensors. *Sensors* **2020**, *20*, 2366.
23. Tang, X.; Wang, X.; Cattley, R.; Gu, F.; Ball, A.D. Energy harvesting technologies for achieving self-powered wireless sensor networks in machine condition monitoring: A review. *Sensors* **2018**, *18*, 4113. [[CrossRef](#)]
24. Toprak, A.; Tigli, O. Piezoelectric energy harvesting: State-of-the-art and challenges. *Appl. Phys. Rev.* **2014**, *1*, 031104. [[CrossRef](#)]
25. Wang, S.; Lin, L.; Wang, Z.L. Triboelectric nanogenerators as self-powered active sensors. *Nano Energy* **2015**, *11*, 436–462. [[CrossRef](#)]
26. Xiao, J.; Zou, X.; Xu, W.Y. ePave: A self-powered wireless sensor for smart and autonomous pavement. *Sensors* **2017**, *17*, 2207. [[CrossRef](#)] [[PubMed](#)]
27. Hasni, H.; Alavi, A.H.; Chatti, K.; Lajnef, N. A Self-Powered Surface Sensing Approach for Detection of Bottom-Up Cracking in Asphalt Concrete Pavements: Theoretical/Numerical Modeling. *Constr. Build. Mater.* **2017**, *144*, 728–746. [[CrossRef](#)]
28. Agorastou, Z.; Kalenteridis, V.; Siskos, S. A 1.02  $\mu$ W Autarkic Threshold-Based Sensing and Energy Harvesting Interface Using a Single Piezoelectric Element. *J. Low Power Electron. Appl.* **2021**, *11*, 27. [[CrossRef](#)]
29. Panayanthatta, N.; Clementi, G.; Ouhabaz, M.; Costanza, M.; Margueron, S.; Bartasyte, A.; Basrou, S.; Bano, E.; Montes, L.; Dehollain, C.; et al. A Self-Powered and Battery-Free Vibrational Energy to Time Converter for Wireless Vibration Monitoring. *Sensors* **2021**, *21*, 7503. [[CrossRef](#)]
30. Gonzalez, A.; Papagiannakis, A.; O'Brien, E. Evaluation of an artificial neural network technique applied to multiple-sensor weigh-in-motion systems. *Transp. Res. Rec. TRB* **2003**, *1855*, 151–159. [[CrossRef](#)]

**Disclaimer/Publisher's Note:** The statements, opinions and data contained in all publications are solely those of the individual author(s) and contributor(s) and not of MDPI and/or the editor(s). MDPI and/or the editor(s) disclaim responsibility for any injury to people or property resulting from any ideas, methods, instructions or products referred to in the content.